# Waterlogging in soil restricts the growth of *Gleditsia sinensis* seedlings and inhibits the accumulation of lignans and phenolic acids in thorns

**Zai-Qi Luo** [1, 2], **Xiao-Qian Shi** [3], **Xian-Ying Wang** [3], **Qiu-Lan Yang** [3], **Xin Pan** [3], **Wen-Xia Pan** [3], **Chun-Li Luo** [3], **Shan-Shan Yu** [3], **Wen-Wen Zhou** [3], **Bin-Rui Ren** [3], **Yin Yi** [1], **Ximin Zhang** [Corresp. 1, 3, 4]

[1] Key Laboratory of State Forestry Administration on Biodiversity Conservation in Karst Area of Southwest, Guizhou Normal University, Guiyang, China

[2] Guizhou Academy of Forestry, Guiyang, China

[3] School of Life Sciences, Guizhou Normal University, Guiyang, Guizhou, China

[4] Key Laboratory of Environment Friendly Management on Alpine Rhododendron Diseases and Pests of Institutions of Higher Learning in Guizhou Province, Guizhou Normal University, Guiyang, China

Corresponding Author: Ximin Zhang
Email address: zhxm409@163.com

*Gleditsia sinensis*, commonly known as Chinese Zaojiao, has important economic value and medicinal compounds in its fruits and thorns, making it widely cultivated artificially in China. However, the available literature on the impact of waterlogging on the growth of *G. sinensis* seedlings and the accumulation of metabolite compounds in its thorns is limited. To address this knowledge gap, *G. sinensis* seedlings were planted in soil supplemented with pindstrup substrate, which enhances the water-holding capacity of the soil. The analyses of biomass and nutrient elements in *G. sinensis* seedlings and metabolite accumulation in its thorns were conducted. The results showed that the waterlogged soil significantly diminished the height, fresh weight, and dry weight of *G. sinensis* seedling roots and stems ($P < 0.05$). Furthermore, waterlogging hindered the uptake of iron (Fe) and manganese (Mn), as well as the transport of potassium (K). The identified metabolites within the thorns were categorized into 16 distinct groups. Relative to the control soil, fatty acids and derivatives were the most down-regulated metabolites in the waterlogged soil, accounting for 40.58% of the total metabolites, followed by lignans (38.71%), phenolic acids (34.48%), saccharides and alcohols (34.15%), steroids (16.67%), alkaloids (12.24%), flavonoids (9.28%), and glycerophospholipids (7.41%). Conversely, nucleotides and derivatives experienced the greatest up-regulation in the waterlogged soil, accounting for 50.00% of the total metabolites. In conclusion, waterlogging negatively impacted the growth of *G. sinensis* seedlings and inhibited the accumulation of metabolites. Hence, when considering the accumulation of secondary metabolites such as lignans and phenolic acids, appropriate management of soil moisture levels should be taken into account.

# Waterlogging in Soil Restricts the Growth of *Gleditsia sinensis* Seedlings and Inhibits the Accumulation of Lignans and Phenolic acids in Thorns

**Zai-Qi Luo[1,4], Xiao-Qian Shi[2], Xian-Ying Wang[2], Qiu-Lan Yang[2], Xin Pan[2], Wen-Xia Pan[2], Chun-Li Luo[2], Shan-Shan Yu[2], Wen-Wen Zhou[2], Bin-Rui Ren[2], Yin Yi[1], Xi-Min Zhang[1,2,3,*]**

[1] Key Laboratory of State Forestry Administration on Biodiversity Conservation in Karst Area of Southwest, Guizhou Normal University, Guiyang 550025, China;
[2] School of Life Sciences, Guizhou Normal University, Guiyang 550025, China;
[3] Key Laboratory of Environment Friendly Management on Alpine Rhododendron Diseases and Pests of Institutions of Higher Learning in Guizhou Province, Guizhou Normal University, Guiyang 550025, China;
[4] Guizhou Academy of Forestry, Guiyang 550025, China

Corresponding Author:
Xi-Min Zhang
School of Life Sciences, Guizhou Normal University, Guiyang 550025, China
Email address: zhxm409@163.com

## Abstract

*Gleditsia sinensis*, commonly known as Chinese Zaojiao, has important economic value and medicinal compounds in its fruits and thorns, making it widely cultivated artificially in China. However, the available literature on the impact of waterlogging on the growth of *G. sinensis* seedlings and the accumulation of metabolite compounds in its thorns is limited. To address this knowledge gap, *G. sinensis* seedlings were planted in soil supplemented with pindstrup substrate, which enhances the water-holding capacity of the soil. The analyses of biomass and nutrient elements in *G. sinensis* seedlings and metabolite accumulation in its thorns were conducted. The results showed that the waterlogged soil significantly diminished the height, fresh weight, and dry weight of *G. sinensis* seedling roots and stems ($P < 0.05$). Furthermore, waterlogging hindered the uptake of iron (Fe) and manganese (Mn), as well as the transport of potassium (K). The identified metabolites within the thorns were categorized into 16 distinct groups. Relative to the control soil, fatty acids and derivatives were the most down-regulated metabolites in the waterlogged soil, accounting for 40.58% of the total metabolites, followed by lignans (38.71%), phenolic acids (34.48%), saccharides and alcohols (34.15%), steroids (16.67%), alkaloids (12.24%), flavonoids (9.28%), and glycerophospholipids (7.41%). Conversely, nucleotides and derivatives experienced the greatest up-regulation in the waterlogged soil, accounting for 50.00% of the total metabolites. In conclusion, waterlogging negatively impacted the growth of *G. sinensis* seedlings and inhibited the accumulation of metabolites. Hence, when considering the accumulation of secondary metabolites such as lignans and phenolic acids, appropriate management of soil moisture levels should be taken into account.


**Keywords:** *Gleditsia sinensis*; water-holding capacity; soil water potential; secondary metabolites; UHPLC-MS

## Introduction

The genus *Gleditsia* Linn. encompasses a diverse array of plants that are classified under the Leguminosae family. These plants boast a global distribution, being found in various regions across Asia, tropical Africa, and the Americas. There are approximately 16 documented species worldwide. Within China, specifically, the genus comprises six distinct species along with two varieties (http://www.iplant.cn/info/Gleditsia?t=foc). These species are primarily distributed

across several provinces, including Hebei, Shanxi, Fujian, Guangdong, Guangxi, Shanxi, Ningxia, Gansu, Sichuan, Guizhou, Yunnan, Shandong, Jiangsu, and Zhejiang (http://www.iplant.cn/info/Gleditsia%20sinensis?t=foc). Among the Gleditsia genus, *Gleditsia sinensis* stands out as a prominent species commonly referred to as Chinese Zaojiao.

*Gleditsia sinensis*, due to its considerable economic value, offers various versatile applications. Its pod yields a juice that serves as an effective substitute for soap in the washing of silk and wool fabrics. Its young shoots, when combined with oil and salt, can be utilized as a culinary ingredient. Additionally, the cooked and candied endosperm of seeds can be consumed directly. Moreover, the dried thorns of *G. sinensis* contain a diverse array of potent medicinal compounds and exert inhibitory effects on the proliferation of colon cancer cells, liver cancer cells, gastric cancer cells, and smooth muscle cells (*Lee et al., 2010*; *Yu et al., 2015*; *Lee et al., 2013*; *Lee et al., 2012*). Consequently, its thorns have gained widespread usage as a herbal medicine in various Asian countries. In traditional Chinese medicine, it is frequently prescribed as an adjunctive therapy for the treatment of breast cancer, lung cancer, and other types of cancer (*Zhang et al., 2016*).

Despite its significant economic value, the *G. sinensis* tree remains relatively scarce, primarily observed in sparsely distributed regions near residential areas. In recent years, the province of Guizhou has initiated efforts to vigorously develop characteristic forestry in support of rural revitalization. For example, in 2021, the cultivation of *G. sinensis* within this province is projected to yield a newly planted area of 20.37 thousand hectares, contributing to a total area of 893 thousand hectares (http://www.forestry.gov.cn/main/5384/20210724/172550581923033.html). Currently, it is known that the species is a deciduous tree that prefers abundant sunlight and has robust tolerance to drought conditions. Remarkably, *G. sinensis* demonstrates adaptability to various soil types, including limestone soil, acidic soil, clay soil, sandy soil, and even slightly saline-alkaline soil (Geyer, 1993; Tilstone et al., 1998). Therefore, understanding the plasticity of this species in facing different abiotic conditions present in the soil can directly contribute to the forestry of this species.

Soil moisture stands as a critical environmental parameter that significantly impacts the normal growth and survival of plants (*Liang et al., 2019*). In recent years, due to climate change, the global hydrological cycle has undergone alterations, resulting in uneven patterns of rainfall

intensity and distribution. Heavy rainfall frequently leads to the saturation of soil moisture, particularly in areas with low-lying terrains, clay-rich soils, or insufficient drainage conditions, ultimately causing a waterlogging stress (*Herzog et al., 2016*; *Pan et al., 2021*). Waterlogging can impede the entry of oxygen into the root system, resulting in hypoxia and root suffocation, which can have adverse effects on plant growth and development. Previous studies have examined the relationships between various environmental factors, such as light exposure, exogenous calcium levels, and drought stress, and the growth of *G. sinensis* (*Liu et al., 2023*; *Guo et al., 2021*; *Yan et al., 2006*). Nevertheless, there is a paucity of research focusing on the impact of waterlogging on the growth of *G. sinensis* seedlings. Consequently, it is necessary to further study the potential effects of waterlogging on the growth of *G. sinensis* seedlings.

Recent scientific literature has witnessed significant contributions regarding the metabolic composition, isolation, and identification of novel compounds extracted from the thorns of *G. sinensis*. Notable examples include Zhang et al. (*2020*), Zeng et al. (*2023*), and Yu et al. (*2017*), who successfully isolated new compounds from *G. sinensis* thorns. In a related study, Ya et al. (*2022*) conducted targeted metabolomics to compare the differences in chemical composition between the epidermis, xylem, and pith of *G. sinensis* thorns. While Liu et al. (*2020*) undertook a comparative investigation of metabolite accumulation in different tissues of *G. sinensis* under conditions of drought stress and rehydration; these studies have not specifically explored the impact of waterlogging on the metabolite accumulation within *G. sinensis* thorns. Hence, the present study aims to provide a comprehensive understanding of both the growth patterns of *G. sinensis* seedlings and the alterations in metabolite accumulation within its thorns in response to excessive water levels in the soil. The primary objective is to analyze the potential influence of waterlogging on the growth of *G. sinensis* seedlings, and specifically identify the types of metabolite biosynthesis that are significantly inhibited in such conditions. By doing so, this research endeavors to shed light on the complex relationship between waterlogging, *G. sinensis* growth dynamics, and the synthesis of key metabolites.

## Materials & Methods

### Determination of Soil ~~substrate and its~~ physical and chemical properties

The soil matrix used in this study was divided into two distinct treatment groups: control soil and pindstrup soil. The control soil consisted of a blend of garden soil (purchased from the flower market in Guiyang city) and humus soil (purchased from Organic Fertilizer Development

Co., Ltd. in Guiyang city) in a 1:1 (v/v) ratio. On the other hand, the pindstrup soil comprised a mixture of garden soil, humus soil, and Pindstrup moss peat substrate (sourced from Pindstrup Company, Ryomgaard (Kongerslev), Denmark) in a ratio of 0.5:0.5:1 (v/v). Under natural conditions, the pindstrup substrate possesses notable water retention capabilities. To facilitate the experiment, the mixture of soils was then placed in black tree planting bags, measuring 25 cm in diameter and 20 cm in height. These bags were equipped with drainage outlets at the bottom. Both types of soil were adequately watered, and the soil moisture within the planting bags was monitored within a controlled greenhouse environment. During the measurement process, soil samples were extracted from a depth of 10 cm, with four points sampled and meticulously blended within each planting bag to form one replicate. The soil water potential was promptly determined using a dew point potential meter (WP4-T, USA). Subsequent to the measurement, the fresh soil samples were immediately weighed, dried at 60°C until reaching a constant weight, and weighed again to determine the dry weight. The soil water content was calculated using the formula: soil water content = (fresh weight - dry weight) / dry weight × 100%. Each treatment was subject to four replicates of soil measurements to ensure statistical robustness.

To examine the disparities in nutrient elements between the two soil types, the nutrient content within each soil was determined. The soil samples were subjected to a series of preparatory steps. Initially, the soil was allowed to air-dry naturally, after which it was ground in a mortar and passed through a 100-mesh sieve to ensure uniform particle size. For further analysis, the samples were digested using microwave-assisted techniques, and the metal element content (such as K, Ca, Mg, Fe, Cu, Zn, Mo, and Mn) was measured using Inductively Coupled Plasma-Mass Spectrometry (ICP-MS) following appropriate filtration methods (*Yu et al., 2014*). The quantification of metal elements was carried out by referencing the standard curve obtained from the analysis of a mixed standard sample of metals (GNM-M1810581-2013). Additionally, the total nitrogen (TN) content of the soil was determined through the $H_2SO_4$–$K_2Cr_2O_7$ method (*Bao, 2020*). By employing the molybdenum blue method (*Liu et al., 2020*), the total phosphorus (TP) content of the soil was also ascertained. The results showed a significantly higher Ca content in the pindstrup soil (31.14 g. $kg^{-1}$) compared to the control soil (13.61 g. $kg^{-1}$). It is speculated that this Ca content might not impact the growth of *G. sinensis* seedlings, as in Karst areas where *G. sinensis* trees thrive, the total Ca content in the soil can reach as high as 40.05 g. $kg^{-1}$ (*Yang et al.,*

*2021*). However, no significant differences were observed in the measured nutrient element contents, including TN, TP, K, Mg, Fe, Cu, Zn, Mo, and Mn (Table S1).

## Seed germination and seedling growth

Mature pods of *G. sinensis* were meticulously collected from Quanhu Park in Guiyang city, located in Guizhou Province (106°62′E, 26°67′N). The harvested *G. sinensis* seeds were carefully selected, ensuring the removal of any infested seeds. These seeds were then placed in a storage cabinet for safekeeping. Prior to planting, the seeds were subjected to a preparatory treatment. Firstly, they were soaked in concentrated sulfuric acid for duration of 2 hours, followed by thorough rinsing with tap water on three separate occasions. Subsequently, the seeds were immersed in tap water at room temperature until they achieved full hydration and experienced notable swelling. The swollen seeds were then planted in the aforementioned tree planting bags, allowing them to grow naturally under ambient conditions for a period of one year before commencing with various measurements.

## Measurement of seedlings biomass

The seedlings were carefully extracted from the planting bags, and the rhizosphere soil was thoroughly rinsed with tap water to remove any adhering debris. Next, the roots were precisely severed at the junction of the roots and stems, and the excess moisture on the roots was carefully blotted using filter paper. The fresh weight of the roots was recorded, after which the roots were dried at a consistent temperature of 60°C until reaching a constant weight, facilitating the determination of the dry weight of the roots. From each seedling, a random selection of four compound leaves was made, and the number of leaflets was accurately recorded. Subsequently, the average number of leaflets was calculated. Additionally, the length of five thorns, located approximately 10 cm from the stem, was meticulously measured from a representative seedling, enabling the determination of the average length of thorns. To further explore the plant's characteristics, all the leaves of a single seedling were excised, and the fresh weight of the leaves was measured. Following this, the leaves were dried at a consistent temperature of 60°C until reaching a constant weight, facilitating the determination of the dry weight. Furthermore, the lateral branches were pruned from a seedling, and the stem was cut off. The fresh weight of the stem was measured. Subsequently, the stem was dried at 60°C until reaching a constant weight, allowing for the determination of the dry weight. To ensure statistical validity, four seedlings were used as biological replicates for each treatment.

## Determination of nutrient elements in plant tissue

The previously dried plant roots, stems, and leaves were subjected to further processing for the purpose of determining the content of nutrient elements. Initially, these dried plant tissues were finely crushed using a grinder and subsequently sieved through a 100-mesh sieve to achieve a uniform and homogeneous particle size distribution. Next, the samples underwent digestion using microwave-assisted techniques, and the resulting digestion solution was filtered prior to analysis. The metal elements present in the digestion solution, including K, Ca, Mg, Fe, Cu, Zn, Mo, and Mn, were quantified using inductively coupled plasma-mass spectrometry (ICP-MS) (*Yu et al., 2014*). To ensure accuracy, the content of these metal elements was determined by referencing a previously established standard curve obtained from the analysis of a mixed standard sample containing metals.

## Metabolite detection of thorns

All of the thorns derived from the stems of a single seedling were meticulously collected for analysis. Each experimental treatment comprised 6 seedlings, ensuring an adequate number of biological replicates. Subsequent to thorn collection, they were promptly transferred to centrifuge tubes and rapidly frozen using liquid nitrogen. The frozen thorns were then stored at a low temperature of -80°C to preserve their integrity. For sample preparation, approximately 20 mg of the thorn samples were accurately weighed. Subsequently, 1000 μL of an extraction solution consisting of methanol, acetonitrile, and water in a volumetric ratio of 2:2:1 (v/v) was added to each sample. The extraction solution contained an internal standard mixture to advance the accuracy and precision of the analysis. To ensure optimal extraction, the samples were subjected to grinding at a frequency of 35 Hz for duration of 4 minutes, followed by sonication for 5 minutes in an ice bath. This grinding and sonication process was repeated three times to enhance the extraction efficiency. After allowing the samples to stand at -40°C for 1 hour, they were subjected to centrifugation at 12000 rpm at 4°C for 15 minutes. The resulting supernatant was carefully collected and utilized for subsequent detection and analysis. To evaluate the repeatability of the analytical method under consistent processing conditions, an equal amount of the supernatant was mixed to create a quality control (QC) sample, which served as a reference for assessing the analytical reproducibility.

The compounds were separated utilizing an UHPLC system (Vanquish, Thermo Fisher Scientific, Wilmington, NC, USA). A Phenomenex Kinetex C18 column with dimensions of

2.1mm×50mm and a particle size of 2.6μm was employed for the chromatographic separation. The mobile phase consisted of two components: mobile phase A, which was a 0.1% acetic acid solution, and mobile phase B, which was a mixture of acetonitrile and isopropanol in a volumetric ratio of 1:1 (v/v). A gradient elution method was employed according to the following time intervals: 0-0.5 min, 1% B; 0.5-4 min, 1%-99% B; 4-4.5 min, 99% B; 4.5-4.55 min, 99%-1% B; 4.55-6 min, 1% B. The column was maintained at a constant temperature of 25°C, while the injection chamber temperature was set to 4°C. The flow rate was set at 0.3 mL/min, and an injection volume of 2 μL was used.

MS (Orbitrap Exploris 120, Thermo Fisher Scientific, Wilmington, NC, USA) combined with control software (Xcalibur, version 4.4, Thermo Fisher Scientific, Wilmington, NC, USA) was employed to facilitate the acquisition of both primary and secondary mass spectrometry data. The instrument configuration adhered to the following precise parameters: - Sheath gas flow rate: 50 Arb - Auxiliary gas flow rate: 15 Arb - Capillary temperature: 320°C - Full MS resolution: 60000 - MS/MS resolution: 15000 - Collision energy: Sequential Normalized Collision Energy (SNCE) set at 20/30/40 - Spray voltage: 3.8 kV (positive ionization mode) or -3.4 kV (negative ionization mode)

## Metabolite identification and data processing of thorns

The raw data obtained from the experiment was processed and converted into mzXML format using the ProteoWizard software. Peak detection and annotation were accomplished through the utilization of an in-house R program and the BiotreeDB database (version 2.1). For multivariate analyses, including orthogonal projections to latent structures-discriminant analysis (OPLS-DA) and principal component analysis (PCA), the MetaboAnalyst 5.0 software platform was employed. In the OPLS-DA analysis, the variable importance in the projection (VIP) value of the first principal component was obtained. Metabolites with a VIP score greater than 1 and a *P*-value less than 0.05 (determined through Student's t-test) were considered to be significantly altered between the experimental groups. Following the identification of differential metabolites, a subsequent Kyoto Encyclopedia of Genes and Genomes (KEGG) enrichment analysis was conducted to gain insights into the biological pathways and processes associated with these metabolites.

## Statistical analysis

The data were presented as mean ± standard deviation (SD) and assessed for statistical significance using independent sample *t*-tests conducted in SPSS version 18 ($P < 0.05$).

## Results

### Pindstrup substrate maintained waterlogging in soil

The water content and water potential of both soil types were continuously monitored for a period of 16 days. The findings revealed a decreasing trend in relative water content for both the control soil and the pindstrup soil. However, at a specific monitoring time point (e.g. the 9$^{th}$ day), the water content of the pindstrup soil (53.14%) was significantly higher than that of the control soil (28.36%) (Figure 1A). In contrast to the results observed for soil water content, the water potential of the pindstrup soil did not display significant changes throughout the 16-day measurement period. Notably, the water potential in the pindstrup soil was found to be significantly higher than that in the control soil (Figure 1B). These results suggest that the pindstrup soil is capable of maintaining a higher level of available water in the soil matrix, even after a prolonged period without regular irrigation.

### Inhibition of seedling growth due to waterlogging

**some morphological traits of the seedlings were…**

After one year of growth, ~~the biomass~~ of seedlings w~~as~~ measured in both soil types. The results revealed significant differences in plant height, stem fresh weight, root fresh weight, stem dry weight, and root dry weight between the control soil (with measurements of 105.53cm, 27.63g, 19.65g, 10.95g, and 6.27g, respectively) and the pindstrup soil (with measurements of 70.66cm, 13.73g, 12.10g, 5.48g, and 3.38g, respectively) ($P < 0.05$) (Figure 2； Table 1). The observed growth phenotypes of the seedlings corroborated the ~~biomass~~ **morphological** data. The integration of soil physical and chemical properties data demonstrated the inhibitory effects of waterlogging on the growth of *G. sinensis* seedlings.

### Influence of waterlogging on the nutrient content of seedlings

To further investigate potential differences in nutrient elements in *G. sinensis* seedlings grown in the two soil types, the contents of nutrient elements in the roots, stems, and leaves of one-year-old seedlings were measured. The results indicated that the contents of Fe and Mn in the roots of seedlings cultivated in the control soil were significantly higher compared to those in the pindstrup soil. Conversely, the contents of Cu and Mo in the roots of seedlings grown in the control soil were significantly lower than those in the pindstrup soil ($P < 0.05$) (Figure 3). In the

stems of seedlings grown in the control soil, the K content was significantly higher than that in the pindstrup soil, while the Mo content was significantly lower ($P < 0.05$) (Figure 3). Furthermore, the Mo content in the leaves of seedlings grown in the control soil was significantly lower than that in the pindstrup soil ($P < 0.05$) (Figure 3); however, no significant differences were found in the contents of other elements.

## Screening and analysis of differentially abundant metabolites in *G. sinensis* thorn

Using the UHPLC- MS detection platform, total ion chromatograms (TIC) of thorn samples were obtained under both positive and negative ion modes for the two treatments (Figure S1). The total ion flow of thorn samples was comparable between the two treatments, but differences in peak area were observed. By matching with the mass spectrometry database (Biotree DB V2.1), a total of 836 metabolites were annotated (Table S2). PCA was performed on all detected metabolites, including quality control samples, to elucidate the variations both between and within treatment groups. The PCA analysis revealed that PC1 and PC2 accounted for 32.1% and 14.6% of the total variation, respectively (Figure 4A). To obtain more reliable differences, OPLS-DA was utilized to filter the orthogonal variables in metabolites. The OPLS-DA successfully distinguished the metabolites of thorn in the control soil from those in the pindstrup soil (Figure 4B). These findings indicate significant differences in the metabolites of thorn grown in the two different soil types.

To further explore the disparities in metabolites between the thorn samples from the control soil and pindstrup soil, differentially abundant metabolites were identified. A total of 265 differentially abundant metabolites (VIP > 1 and a *P*-value < 0.05) were screened between the thorn of pindstrup soil and control soil, and visualized through a heat map (Figure 4C). Compared to the control soil, 67 metabolites were up-regulated, while 198 metabolites were down-regulated in the thorn of pindstrup soil (Figure 4C, Table S3).

To investigate the impact of waterlogging on metabolite accumulation, the detected metabolites were classified into 16 categories (Table 2). Among the down-regulated metabolites, the most abundant category was Fatty acids and derivatives, accounting for 40.58%, followed by lignans (38.71%), phenolic acids (34.48%), saccharides and alcohols (34.15%), steroids (16.67%), alkaloids (12.24%), flavonoids (9.28%), and glycerophospholipids (7.41%) (Table 2). Among the up-regulated metabolites, the most abundant category was nucleotides and derivatives, accounting for 50.00%, followed by glycerophospholipids (18.52%) and steroids

(13.89%) (Table 2). Overall, these results also indicated a more pronounced effect of waterlogging on the primary metabolites of *G. sinensis* thorn.

## Enrichment analysis of differentially abundant metabolites

To identify the key metabolic pathways affected by waterlogging, the differentially abundant metabolites were matched to the KEGG database for enrichment analysis. Overall, these metabolites were found to be involved in 66 KEGG pathways, including metabolic pathways and biosynthesis of secondary metabolites (Table S4). Among these pathways, metabolic pathways, phenylalanine metabolism, phenylpropanoid biosynthesis, linoleic acid metabolism, tyrosine metabolism, tryptophan metabolism, ABC transporters, citrate cycle, lysine degradation, glyoxylate and dicarboxylate metabolism, cutin, suberine and wax biosynthesis, ubiquinone and other terpenoid-quinone biosynthesis, pyruvate metabolism, sulfur metabolism, and phenylalanine, tyrosine, and tryptophan biosynthesis showed significant enrichment ($P < 0.05$) (Figure 5). Notably, a significant number of the identified metabolic pathways were associated with amino acid biosynthesis and metabolism, indicating a substantial impact of waterlogging on these pathways.

# Discussion

Roots serve as the primary interface between plants and the soil, making them highly susceptible to water stress. Our findings showed that the pindstrup soil had significantly higher water content and soil water potential compared to the control soil after a two-week non-irrigation period (Figure 1). These results suggested that pindstrup soil has high water retention capacity and will accumulate more water in the rhizosphere (*Song et al., 2016*; *Carminati & Vetterlein, 2012*), resulting in waterlogged stress for the *G. sinensis* seedlings during the growth stage. As our results demonstrate, in the pindstrup soil (excessive moisture), the fresh weight and dry weight of *G. sinensis* seedling roots were significantly lower compared to those in the control soil (Figure 2 and Table 1), indicating inhibited root growth. In fact, certain drought-tolerant or waterlogging-sensitive species, such as *Quercus robur, Liquidambar styraciflua*, and *Lupinus angustifolius* (*Kreuzwieser & Rennenberg, 2015*; *Schmull & Thomas， 2000*； *Neatrour et al., 2007*; *Bramley et al., 2011*; *Colin-Belgrand, Dreyer & Biron, 1991*), also experience inhibited root growth due to waterlogging. This was consistent with our results, suggesting that *G. sinensis* is a potential drought-tolerant species (*Liu et al., 2020*). Additionally, *G. sinensis* seedlings in the pindstrup

soil showed a decrease in thorn length, leaflet number, stem diameter, leaf fresh weight, and leaf dry weight, especially significantly reduced plant height, stem fresh weight, and stem dry weight (Figure 2 and Table 1). This is explained by the limitation of root biomass reduction caused by waterlogging, which has a significant impact on plant growth patterns (*Schmull & Thomas， 2000*).

Waterlogged trees often experience impaired nutrient absorption and transportation from roots to stems (*Schmull & Thomas， 2000*; *Merchant et al., 2010*). Our research results indicated that levels of Fe and Mn in *G. sinensis* roots exposed to waterlogging soil were significantly reduced (Figure 3). This are attributed to root hypoxia caused by waterlogging, which hinders the entry of Fe and Mn into the roots (*Jiménez et al., 2021*), as well as reduced activities of proton ATPase and ferric chelate reductase (FCR) due to waterlogging, leading to decreased Fe and Mn uptake (*Martinea-Cuenca et al., 2015*). In contrast, Cu and Mo levels increased in roots grown in waterlogged soil, which are explained by enhancing Cu absorption and contributing to increased superoxide dismutase (SOD) activity to maintain the balance of reactive oxygen species within the plant (*Chen et al., 2011*). Additionally, Mo uptake may activate root defense mechanisms to counteract damage caused by waterlogging stress on the roots (*Hayyawi et al., 2020*; *Heshmat et al., 2021*). K levels in stems were significantly lower than in control soil, indicating that waterlogging had the greatest impact on inhibiting potassium transport from roots to stems. In Pindstrup soil, Mo levels increased in stems and leaves, likely due to significant uptake and accumulation of Mo by the roots (Figure 3G).

Some studies have reported the chemical composition of thorn using metabolomics methods (*Ya et al., 2022*; *Bai et al., 2023*). In our current study, a comprehensive analysis identified a total of 836 putative metabolites in the thorn (Supplementary Table 2). Fatty acids play essential roles as precursors of cuticular waxes in the plant cuticle and are specific to various membrane lipids, contributing to membrane homeostasis. It has been reported by Ya et al. (*2022*) that fatty acids accounted for a considerable proportion of the thorn metabolites and may contribute to its hardness (*Ya et al., 2022*). However, in waterlogging soil, the levels of fatty acids and their derivatives were down-regulated, suggesting that this may affect the synthesis of cuticular waxes in *G. sinensis* thorn, thereby reducing their hardness. Lignans, secondary metabolites derived from phenylpropanoids, have been recognized for their bioactive properties in various human diseases, including colon and breast cancer (*Záleák, Bon & Pospíil, 2019*). Additionally,

phenolic acids, another group of secondary metabolites, have shown potential as anticancer compounds, with many acting as cytotoxic agents that promote apoptosis, inhibit proliferation, and target cancer cells (*Abotaleb et al., 2020*). Importantly, our findings showed that waterlogging soil significantly decreased the accumulation of lignans and phenolic acids. There results suggest that soil moisture levels should be considered when utilizing these metabolites for future disease treatments.

There are variations in carbohydrate accumulation among different species. Jaeger et al. (*2009*) reported a significant decrease in carbohydrate content in waterlogging-sensitive plants. Consistent with these findings, our results indicate that carbohydrate accumulation was down-regulated in waterlogging soil (Table 2), indicating that *G. sinensis* may be a waterlogging-sensitive species from a carbohydrate perspective. Our results observed the accumulation of nucleotides and their derivative metabolites in waterlogging soil (Table 2). This is explained by the the decrease in amino acid content produced by glycolysis due to waterlogging, resulting in a decrease in the number of amino acids entering the tricarboxylic acid (TCA) cycle intermediates (*Kreuzwieser et al., 2009*) and nicotinamide adenine dinucleotide phosphate (NADP) consumption. Nucleotide substances need to be resynthesized to maintain the nucleotide pool homeostasis, thereby replenishing energy deficiency (*Kreuzwieser & Rennenberg, 2015*; *Noctort, Queval & Gakière, 2006*). Sterols and glycerophospholipids are important constituents of cell membranes and membrane lipids in plants. They play essential roles in membrane asymmetry, diversity, and various physiological and biochemical processes related to plant development and stress response (*Du et al., 2022*; *Vijayakumar et al., 2015*). Interestingly, the levels of sterols and glycerophospholipids were up-regulated in waterlogging soil. This indicates that waterlogging may cause damage to cell membranes and membrane lipids, by accumulating sterols and glycerol phospholipids to repair cell membranes and maintain ~~module~~ **their** integrity, thereby enhancing plant resistance.

## Conclusions

Soil amended with pindstrup substrate exhibits a higher water holding capacity, resulting in waterlogging in the soil even after irrigation has ceased in the short term. The waterlogged soil significantly inhibits the growth of roots and stems in *G. sinensis* seedlings. Moreover, it is likely that waterlogging hampers the uptake of Fe and Mn by the roots, impedes the transportation of K

from the roots to the stems, and triggers defense mechanisms for Mo absorption. The primary metabolites in thorn grown in waterlogged soil, such as fatty acids and their derivatives, as well as the secondary metabolites, including lignans and phenolic acids, are predominantly suppressed. Hence, when it becomes necessary to acquire these metabolites from the thorns of *G. sinensis*, careful attention must be given to avoid planting trees in high moisture soil and to soil moisture management.

### Abbreviations

UHPLC-MS: ultra-high performance liquid chromatography-mass spectrometry; TN: total nitrogen; TP: total phosphorus; K: potassium; Ca: calcium; Mg: magnesium; Fe: iron; Cu: copper; Zn: zinc; Mo: molybdenum; Mn: manganese; ICP-MS: inductively coupled plasma-mass spectrometry; QC: quality control; SNCE: Sequential Normalized Collision Energy; OPLS-DA: orthogonal projections to latent structures-discriminant analysis; PCA: principal component analysis; VIP: variable importance in the projection; KEGG: Kyoto Encyclopedia of Genes and Genomes; SD: standard deviation; TIC: total ion chromatograms; PM: primary metabolites; SM: secondary metabolites; FCR: ferric-chelate reductase; SOD: superoxide dismutase; TCA: tricarboxylic acid; NADP: nicotinamide adenine dinucleotide phosphate.

## Acknowledgements

The authors would like to thank the editors and the anonymous reviewers for their constructive comments and suggestions, which helped to improve the quality of this paper.

## Additional Information and Declarations

### Funding

This study was financially supported by the Guizhou Science and Technology Support Plan Project [2021]224; Joint Fund of the Natural Science Foundation of China and the Karst Science Research Center of Guizhou Province (Grant No. U1812401); the Natural Science Foundation of China (NSFC) (32260393); Key Laboratory of Environment Friendly Management on Alpine Rhododendron Diseases and Pests of Institutions of Higher Learning in Guizhou Province ([2022]044); Guizhou Science and Technology Foundation ([2020]1Y130); and the Higher Education Science and Research Youth Project of Guizhou Education Department ([2022]130).

### Competing Interests

The authors declare there are no competing interests.

### Author Contributions

Z.-Q.L. and X.-M.Z. conceived and designed the analysis and wrote and reviewed the paper.
X.-Q.S., X.-Y.W., Q.-L.Y., X.P., W.-X.P., C.-L.L., S.-S.Y., W.-W.Z., and B.-R.R. collected the data and performed the experiment.
X.-Q.S. and X.-M.Z. carried out analysis of the LC-MS.
Z.-Q.L. and X.-M.Z. wrote the original draft.
Y.Y. reviewed the paper. All authors have read and agreed to the published version of the manuscript.

**Data Availability Statement:**

The data presented in this study are available on request from the corresponding author.

**Supplementary Materials:**

The following supporting information can be downloaded at: www., Table S1: All annotated metabolites are detected by UHPLC-OE-MS platform, Table S2: The differentially abuntant metabolites detected by UHPLC-OE-MS in pindstrup soil versus control soil, Table S3: The enrichment analysis of differentially abundant metabolites

## References

**Abotaleb M, Liskova A, Kubatka P, Büsselberg D. 2020.** Therapeutic potential of plant phenolic acids in the treatment of cancer. *Biomolecules* **10**: 221.

**Bai J, Jing X, Yang Y, Wang X, Feng Y, Ge F, Li J, Yao M. 2023.** Comprehensive profiling of chemical composition of *Gleditsiae spina* using ultra-high-performance liquid chromatography coupled with electrospray ionization quadrupole time-of-flight mass spectrometry. *Rapid Communication Mass Spectrometry* **37**: e9467.

**Bao SD. 2020**. Soil agrochemical analysis. China Agriculture Press, Beijing, China.

**Bramley H, Tyerman SD, Turner DW, Turner NC. 2011**. Root growth of lupins is more sensitive to waterlogging than wheat. *Functional Plant Biology* **38**: 910–918.

**Carminati A, Vetterlein D. 2012**. Plasticity of rhizosphere hydraulic properties as a key for efficient utilization of scarce resources. *Annals of Botany* **112**: 277–290.

**Chen CC, Chen YY, Yeh KC. 2011.** Effect of Cu content on the activity of Cu/ZnSOD1 in the Arabidopsis SUMO E3 ligase siz1 mutant. *Plant Signaling Behavior* **6**: 1428-1430.

**Colin-Belgrand M, Dreyer E, Biron P. 1991.** Sensitivity of seedlings from different oak species to waterlogging: effects on root growth and mineral nutrition. *Annals of Forest*

*Science* **48**: 193-204.

**Du Y, Fu X, Chu Y, Wu P, Liu Y, Ma L, Tian H, Zhu B. 2022.** Biosynthesis and the roles of plant sterols in development and stress responses. *International Journal of Molecular Sciences* **23**: 2332.

**Geyer WA. 1993.** Influence of environmental factors on woody biomass productivity in the central great plains U.S.A. *Biomass & Bioenergy* **4**:333–337.

**Guo Y, Liu Y, Zhang Y, Liu J, Gul Z, Guo XR, Abozeid A, Tang ZH. 2021.** Effects of exogenous calcium on adaptive growth, photosynthesis, ion homeostasis and phenolics of *Gleditsia sinensis* Lam. plants under salt stress. *Agriculture* **11**: 978.

**Hayyawi NJH, Al-Issawi MH, Alrajhi AA, Al-Shmgani H, Rihan H. 2020.** Molybdenum induces growth, yield, and defence system mechanisms of the mung bean (*Vigna radiata* L.) under water stress conditions. *International Journal of Agronomy* **2020**: 8887329.

**Herzog M, Striker GG, Colmer TD, Pedersen O. 2016.** Mechanisms of waterlogging tolerance in wheat–a review of root and shoot physiology. *Plant Cell & Environment* **39**: 1068–1086.

**Heshmat K, Lajayer BA, Shakiba MR, Astatkie T. 2021.** Assessment of physiological traits of common bean cultivars in response to water stress and molybdenum levels. *Journal of Plant Nutrition* **44**: 366–372.

**Jaeger C, Gessler A, Biller S, Rennenberg H, Kreuzwieser J. 2009.** Differences in C metabolism of ash species and provenances as a consequence of root oxygen deprivation by waterlogging. *Journal of Experimental Botany* **60**: 4335–4345.

**Jiménez JC, Clode PL, Signorelli S, Veneklaas EJ, Colmer TD, Kotula L. 2021.** The barrier to radial oxygen loss impedes the apoplastic entry of iron into the roots of *Urochloa humidicola*. *Journal of Experimental Botany* **72**: 3279–3293.

**Kreuzwieser J, Hauberg J, Howell KA, Carroll A, Rennenberg H, Millar AH, Whelan J. 2009.** Differential response of gray poplar leaves and roots underpins stress adaptation during Hypoxia. *Plant Physiology* **149**: 461–473.

**Kreuzwieser J, Rennenberg H. 2015.** Molecular and physiological responses of trees to waterlogging stress. *Plant Cell & Environment* **37**: 2245–2259.

**Lee SJ, Park K, Ha SD, Kim WJ, Moon SK. 2010.** *Gleditsia sinensis* thorn extract inhibits human colon cancer cells: the role of ERK1/2, G2/M-phase cell cycle arrest and p53

expression. *Phytotherapy Research* **24**: 1870–1876.

**Lee SJ, Park SS, Kim WJ, Moon SK. 2012.** *Gleditsia sinensis* thorn extract inhibits proliferation and TNF-α-induced MMP-9 expression in vascular smooth muscle cells. *The American Journal of Chinese Medicine* **40**: 373–386.

**Lee SJ, Ryu DH, Jang LC, Cho SC, Kim WJ, Moon SK. 2013.** Suppressive effects of an ethanol extract of *Gleditsia sinensis* thorns on human SNU-5 gastric cancer cells. *Oncology Reports* **29**: 1609–1616.

**Liang H, Xue Y, Shi J, Li Z, Fu B. 2019.** Soil moisture dynamics under *Caragana korshinskii* shrubs of different ages in Wuzhai County on the Loess Plateau, China. *Earth & Environmental Science Transactions of the Royal Society of Edinburgh* **109**: 387–396.

**Liu Q, Mu XM, Zhao GJ, Gao P, Sun WY. 2020.** Effects of fertilization on soil water use efficiency and crop yield on the Loess Plateau, China. *Applied Ecology & Environmental Research* **18**: 6555–6568.

**Liu BS, Meng C, Wang XR, Luo J, Zhao Y. 2023.** Effects of light intensity on morphological structure and physiological characteristics of *Gleditsia sinensis* seedlings. *Russian Journal Plant Physiology* **69**: 164.

**Liu J, Kang R, Liu Y, Wu KX, Tang ZH. 2020.** Differential metabolite accumulation in different tissues of *Gleditsia sinensis* under water stress and rehydration conditions. *Forests* **11**: 542.

**Martínez-Cuenca MR, Quiñones A, Primo-Millo E, Forner-Giner MA. 2015.** Flooding impairs Fe uptake and distribution in citrus uue to the strong down-regulation of genes involved in strategy I responses to Fe deficiency in roots. *Plos One* **10**: e0123644.

**Merchant A, Peuke AD, Keitel C, Macfarlane C, Warren CR, Adams MA. 2010.** Phloem sap and leaf δ13C, carbohydrates, and amino acid concentrations in *Eucalyptus globulus* change systematically according to flooding and water deficit treatment. *Journal of Experimental Botany* **61**: 1785–1793.

**Neatrour MA, Jones RH, Golladay SW. 2007.** Response of three floodplain tree species to spatial heterogeneity in soil oxygen and nutrients. *Journal of Ecology* **95**: 1274–1283.

**Noctort G, Queval G, Gakière B. 2006.** NAD(P) synthesis and pyridine nucleotide cycling in plants and their potential importance in stress conditions. *Journal of Experimental Botany* **57**: 1603.

**Pan J, Sharif R, Xu X, Chen X. 2021.** Mechanisms of waterlogging tolerance in plants: research progress and prospects. *Frontiers in Plant Science* **11**: 627331.

**Schmull M & Thomas FM. 2000.** Morphological and physiological reactions of young deciduous trees (*Quercus robur* L., *Q. petraea*, *Fagus sylvatica* L.) to waterlogging. *Plant & Soil* **225**: 227–242.

**Song Q, Xiao H, Xiao X, Zhu XG. 2016.** A new canopy photosynthesis and transpiration measurement system (CAPTS) for canopy gas exchange research. *Agricultural & Forest Meteorology* **217**: 101–107.

**Tilstone GH, Pasiecznik NM, Harris PJC, Wainwright SJ. 1998.** The growth of multipurpose tree species in the almeria province of spain and its relationship to native plant communities. *International Tree Crops Journal* **9**: 247–259.

**Vijayakumar V, Liebisch G, Buer B, Xue L, Gerlach N, Blau S, Schmitz J, Bucher M. 2015.** Integrated multi-omics analysis supports role of lysophosphatidylcholine and related glycerophospholipids in the *Lotus japonicus*-*Glomus intraradices* mycorrhizal symbiosis. *Plant Cell & Environment* **39**: 393–415.

**Ya H, Li H, Liu X, Chen Y, Zhang J, Xie Y, Wang M, Xie W, Li S. 2022.** Profiling of widely targeted metabolomics for the identification of chemical composition in epidermis, xylem and pith of Gleditsiae Spina. *Biomedical Chromatography* **36**: e5331.

**Yan LI, Gao SM, Ju KY, Li X. 2006.** Physiological and biochemical responses of *Gleditsia sinensis* seedlings to drought stress. *Journal South China Agricultural University* **27**: 66–69.

**Yang ST, Li X, Lou H, Luo Y, Li C, Wang P, Wu X, Zhang J. 2021.** Spatial estimation model and migration analysis of soil total calcium content in the Maolan karst area, Guizhou Province. *Carsologica Sinica* **40**: 449–458.

**Yu J, Xian Y, Li G, Wang D, Zhou H, Wang X. 2017.** One new flavanocoumarin from the thorns of *Gleditsia sinensis*. *Natural Product Research* **31**: 275–280.

**Yu JQ, Xian YX, Geng YL, Wang DJ, Zhou HL, Wang X. 2015.** Anti-liver cancer constituents from the thorns of *Gleditsia sinensis*. *Phytochemistry Letters* **13**: 343–347.

**Yu NJ, Yu J, Zhang W, Cao Y, Zhang TH, Wang YQ. 2014.** Determination of trace elements in different parts of Boju and root soil by ICP-MS. *Journal of Chinese Medical Materials* **37**: 2136-2139.

**Záleák F, Bon JYD, Pospíil J. 2019.** Lignans and neolignans: plant secondary metabolites as a

reservoir of biologically active substances. *Pharmacological Research* **146**: 104284.

**Zeng M, Qi M, Kan Y, Zheng X, Feng W. 2023.** A new flavonoid from the thorn of *Gleditsia sinensis* Lam. *Natural Product Research* **37**: 283–288.

**Zhang JP, Tian XH, Yang YX, Liu QX, Wang Q, Chen LP, Li HL, Zhang WD. 2016.** Gleditsia species: An ethnomedical, phytochemical and pharmacological overview. *Journal of Ethnopharmacology* **178**: 155–171.

**Zhang YB, Lam KH, Chen LF, Wan H, Wang GC, Lee KF, Yip CW, Liu KH, Leung PH, Chan HY. 2020.** Chemical constituents from the thorns of *Gleditsia sinensis* and their cytotoxic activities. *Journal of Asian Natural Product Research* **22**: 1121–1129.

## Figure 1(on next page)

Figure 1, Figure 2, Figure 3, Figure 4, Figure 5

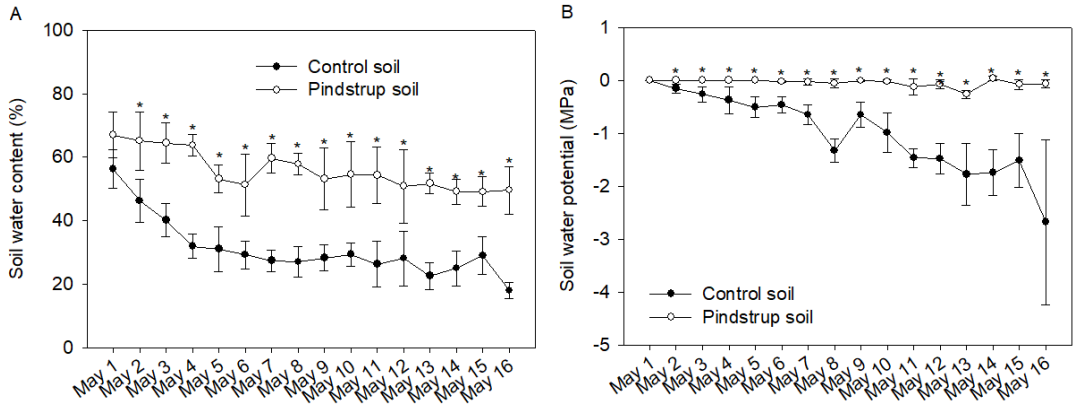


**Figure 1**. Soil water content (**A**) and soil water potential (**B**) in control soil and pindstrup soil. The data represent the mean ± SD (n = 4). Asterisks represent significant differences between contrast soil and pindstrup soil in the same day ($P < 0.05$).

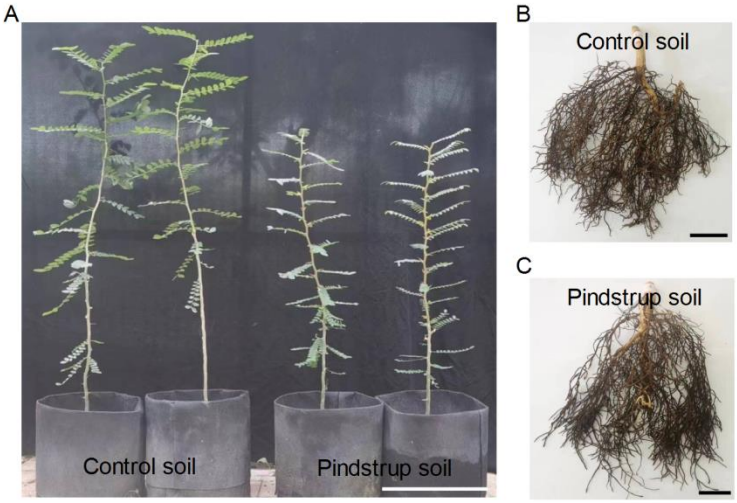


**Figure 2**. The growth phenotypes of *G. sinensis* seedlings grown in control soil and pindstrup soil. (**A**) show the ~~plant~~ height of one-year *G. sinensis* seedlings growing in two types of soil. Bar = 20 cm. (**B**) and (**C**) show~~s~~ the root~~s~~ growth of one-year *G. sinensis* seedlings growing in control soil and pindstrup soil, respectively. Bar = 2 cm.

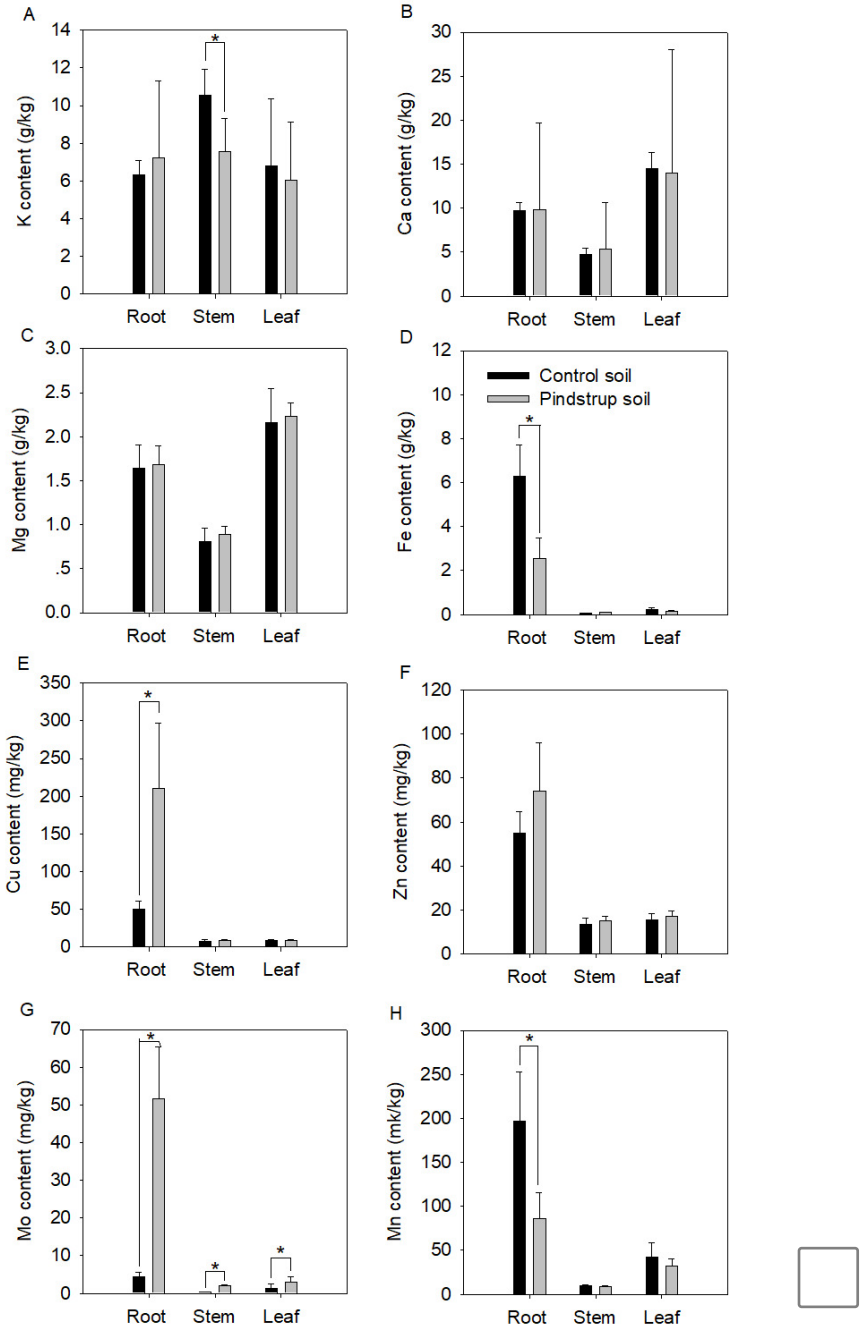


**Figure 3**. K content (**A**), Ca content (**B**), Mg content (**C**), Fe content (**D**), Cu content (**E**), Zn content (**F**), Mo content (**G**), Mn content (**H**) of root, stem and leaf in one-year *G. sinensis* seedlings growing in control soil and pindstrup soil. The data represent the mean ± SD (n = 4). Asterisks represent significant differences between ~~contrast~~ **control** soil and pindstrup soil in the same day ($P < 0.05$).

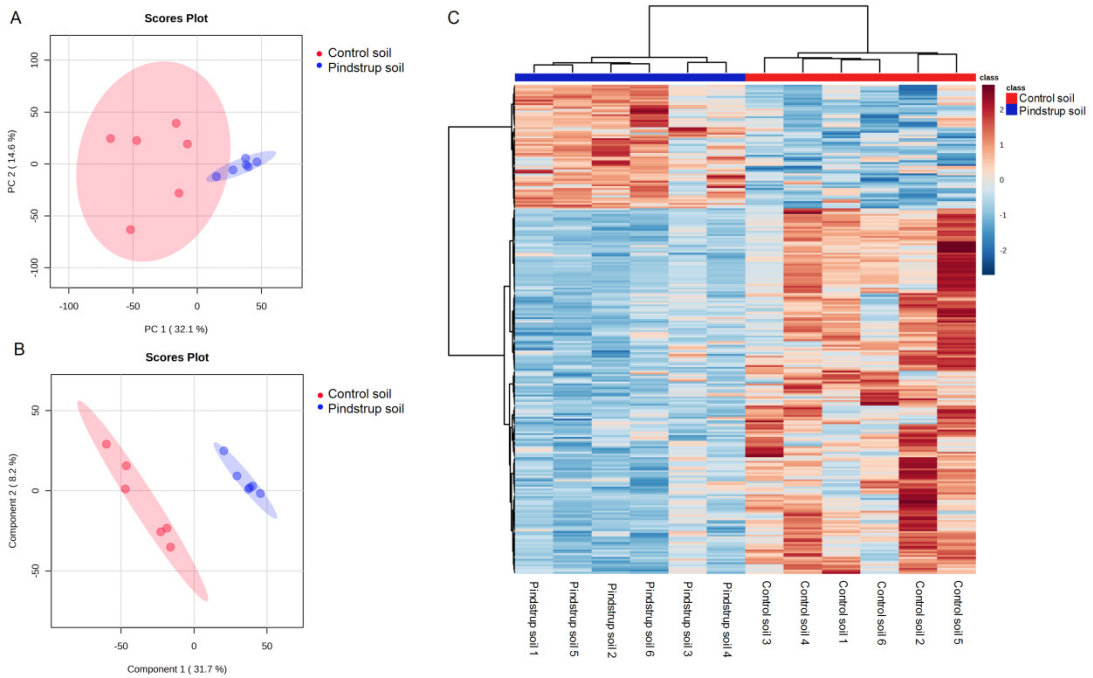


**Figure 4**. Metabolite identification of thorns in *G. sinensis*. (**A**) PCA of samples with six biological repetitions. (**B**) OPLS-DA of samples with six biological repetitions. The red and blue circles display 95% confidence regions of control soil and pindstrup soil. (**C**) Hierarchical clustering analysis of the identified **of** metabolites from thorns ~~in~~ *G. sinensis* grown in control soil and pindstrup soil. Columns and rows represent individual metabolites and different samples, respectively.

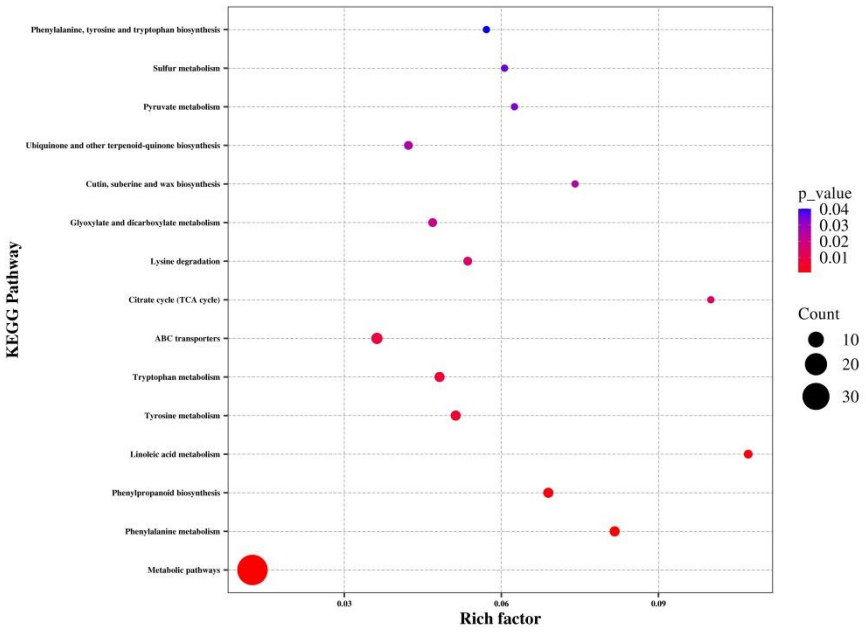


**Figure 5**. KEGG pathway analysis of differentially abundant metabolites of the thorns in *G. sinensis* based on pathway-matched metabolites.

## Table 1(on next page)

Table 1 and Table 2

## Morphological traits

**Table 1** ~~Biomass~~ of seedlings grown in control soil and pindstrup soil.

| ~~Biomass~~ | Control soil | Pindstrup soil |
|---|---|---|
| Plant height (cm) | 105.53±13.52a | 70.66±10.87b |
| Thorn length (cm) | 2.36±0.24a | 1.98±0.44a |
| Leaflet number (N) | 13.75±2.87a | 13.50±2.38a |
| Stem diameter (cm) | 0.71±0.12a | 0.64±0.08a |
| Leaf fresh weight (g) | 14.98±3.11a | 10.07±2.85a |
| Stem fresh weight (g) | 27.63±8.34a | 13.73±5.06b |
| Root fresh weight (g) | 19.65±4.98a | 12.10±2.88b |
| Leaf dry weight (g) | 4.86±1.09a | 3.22±0.89a |
| Stem dry weight (g) | 10.95±3.60a | 5.48±1.92b |
| Root dry weight (g) | 6.27±1.74a | 3.38±1.04b |

The data represent the mean ± SD (n = 4). Different lowercase letters in the same line represent significant differences between contrast soil and pindstrup soil ($P < 0.05$).

**Table 2** Statistics of differentially abundant metabolites of thorns in *G. sinensis* between pindstrup soil versus control soil.

| Primary classification | Type | Number of identified metabolites | Number of down-regulated metabolites | Ratio | Number of up-regulated metabolites | Ratio |
|---|---|---|---|---|---|---|
| Amino acids and derivatives | PM | 49 | 12 | 24.49% | 3 | 6.12% |
| Nucleotides and derivatives | PM | 10 | 2 | 20.00% | 5 | 50.00% |
| Organic acids and derivatives | PM | 82 | 22 | 26.83% | 7 | 8.54% |
| Steroids | PM | 36 | 6 | 16.67% | 5 | 13.89% |
| Saccharides and alcohols | PM | 41 | 14 | 34.15% | 3 | 7.32% |
| Glycerophospholipids | PM | 54 | 4 | 7.41% | 10 | 18.52% |
| Fatty acids and derivatives | PM | 69 | 28 | 40.58% | 4 | 5.80% |
| Alkaloids | SM | 49 | 6 | 12.24% | 2 | 4.08% |
| Coumarins | SM | 36 | 8 | 22.22% | 1 | 2.78% |
| Flavonoids | SM | 97 | 9 | 9.28% | 4 | 4.12% |
| Isoflavonoids | SM | 15 | 4 | 26.67% | 2 | 13.33% |
| Lignans | SM | 31 | 12 | 38.71% | 0 | 0.00% |
| Phenolic acids | SM | 87 | 30 | 34.48% | 3 | 3.45% |
| Tannins | SM | 9 | 2 | 22.22% | 0 | 0.00% |
| Terpenoids | SM | 74 | 14 | 18.92% | 8 | 10.81% |
| Others | SM | 97 | 25 | 25.77% | 10 | 10.31% |
| Total | | 836 | 198 | | 67 | |

PM indicates primary metabolites; SM indicates secondary metabolites.